59th Annual Technical Conference Proceedings
Indianapolis, Indiana, May 9–13, 2016
https://doi.org/10.14332/svc16.proc.0006

© 2016 Society of Vacuum Coaters
All rights reserved. ISSN 0737-5921
www.svc.org

High-Rate Reactive High-Power Impulse Magnetron Sputter Deposition: Principles and Applications

J. Vlcek, J. Rezek, A. Belosludtsev, T. Kozak
Department of Physics and NTIS – European Centre of Excellence
University of West Bohemia, Czech Republic

ABSTRACT

High-power impulse magnetron sputtering with a pulsed reactive gas flow control was used for high-rate reactive depositions of densified, highly optically transparent, stoichiometric ZrO_2 and HfO_2 films on floating substrates. The depositions were performed using a strongly unbalanced magnetron with a planar Zr and Hf target of 100 mm diameter in argon-oxygen gas mixtures at a total pressure close to 2 Pa. The repetition frequency was 500 Hz at the deposition-averaged target power density close to 30 Wcm^{-2} and 50 Wcm^{-2} with voltage pulse durations ranging from 50 µs to 200 µs (the duty cycles from 2.5 % to 10 %). The target-to-substrate distance was 100 mm. For the same duty cycle of 10 %, the deposition rates were up to 120 nm/min for the ZrO_2 films and even up to 345 nm/min for the HfO_2 films. An effective feedback pulsed reactive gas flow control and a simplified relation for the deposition rate of films prepared using a reactive high-power impulse magnetron sputtering are presented.

INTRODUCTION

In spite of several successful applications of the high-power impulse magnetron sputtering (HiPIMS) systems for reactive sputter depositions of dielectric films (see, for example, [1] and the works cited therein), there are still substantial problems with arcing on target surfaces during the reactive deposition processes at high target power densities, particularly for voltage pulses longer than 40 µs, and with low deposition rates achieved.

In the present paper, we report on high-rate reactive depositions of densified stoichiometric dielectric oxide films using HiPIMS with a pulsed reactive gas flow control (RGFC).

SPUTTER DEPOSITION WITH PULSED REACTIVE GAS FLOW CONTROL

The films were deposited using a strongly unbalanced magnetron source with a directly water-cooled planar zirconium, tantalum, or hafnium target (99.9 % Zr, Ta and Hf purity, 100 mm diameter and 6 mm thickness) in a standard stainless steel vacuum chamber [2]. The base pressure before deposition was 10^{-3} Pa. The magnetron was driven by a high-power pulsed DC power supply (HMP 2/1, Hüttinger Elektronik). The repetition frequency, f_r, was 500 Hz, and the pulse duration, t_{on}, ranged from 50 µs to 200 µs with the corresponding duty cycle t_{on}/T_p = 2.5%-10%, where the pulse period $T_p = 1/f_r$. The films were deposited onto silicon substrates at a floating potential. The target-to-substrate distance, d, was 100 mm. The substrate temperature, T_s, reached during depositions without an external heater, was less than 130°C for the ZrO_2 films and less than 165°C for the HfO_2 films.

A reactive gas (oxygen) was admitted into the vacuum chamber from a source via mass flow controllers and two corundum conduits (Figure 1). Two O_2 inlets with a diameter of 1 mm were placed symmetrically above the target racetrack at the same distance from the target surface and oriented to the substrate. The to-substrate O_2 injection in front of the target results in a substantially decreased compound fraction in the target surface layer [3], leading to reduced arcing, increased sputtering of metal atoms, and lower production of O^- ions at the target [1], and in a substantially increased compound fraction in the substrate layer due to a significantly increased flux of O atoms onto the substrate [3]. This is caused by two to three times increased local oxygen partial pressure in front of the O_2 inlets and by a very high degree of dissociation of O_2 molecules in a high-density plasma in front of the target.

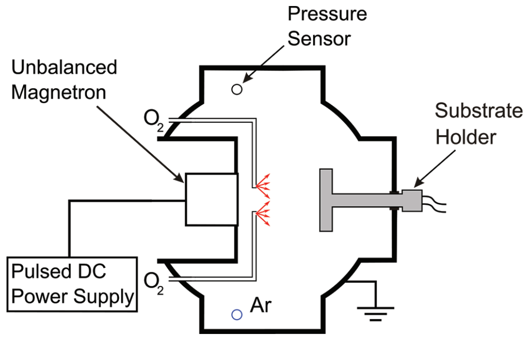

Figure 1. Schematic diagram of the deposition device with two O_2 inlets in front of the target. Also shown are the positions of the pressure sensor and the Ar inlet in the back side of the vacuum chamber.

Waveforms of the magnetron voltage, $U_d(t)$, and the discharge current, $I_d(t)$, were monitored [1], and our own software evaluated the time-varying (the oxygen partial pressure oscillates in the chamber) average target power density in a discharge pulse, S_{da}, given by:

$$S_{da} = \frac{1}{t_{on}} \int_0^{t_{on}} U_d(t) J_t(t) dt. \quad (1)$$

Here, the target current density $J_t(t) = I_d(t)/A_t$, where A_t is the total area of the target (78.54 cm^2 in our case). The deposition-averaged target power density, $<S_d>$, was evaluated with the use of the formula:

$$< S_d >= \frac{1}{t_e - t_s} \int_{t_s}^{t_e} U_d(t) J_t(t) dt, \quad (2)$$

where t_s and t_e are the start and end times of the deposition. The time-varying average discharge current in a period of the power supply, $\bar{I}_d$, was evaluated using the formula:

$$\bar{I}_d = \frac{1}{T_p} \int_0^{T_p} I_d(t) dt. \quad (3)$$

Prior to deposition, we set the nominal target power at an essentially constant magnetron voltage during discharge pulses. Furthermore, we preset the argon partial pressure, p_{ar}, and the total oxygen flow rates in both conduits, Φ_{ox}. Also, we set a pre-selected critical value of the average discharge current in a period of the power supply, $\bar{I}_d(t)$, or the partial pressure of oxygen in the chamber, $p_{ox}(t)$, which were chosen to be the control process parameters (Figures 2 and 3). During the deposition, a process controller provides a control feedback signal to the two O_2 mass flow controllers to adjust the pulsed O_2 flow rate into the vacuum chamber. This is achieved by adjusting the duration of the O_2 flow rate

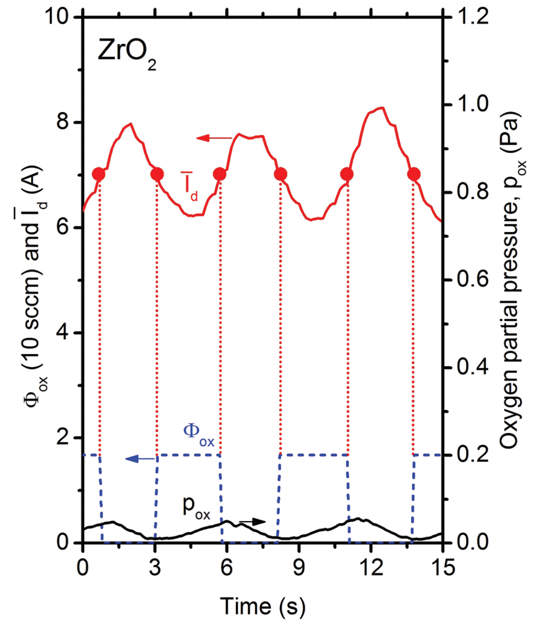

Figure 2. Time evolution of the average discharge current in a period of the power supply, $\bar{I}_d$, oxygen partial pressure, p_{ox}, and the corresponding oxygen flow rate pulses, Φ_{ox}, during a controlled reactive sputter deposition of the stoichiometric ZrO_2 film at $<S_d>$ = 52 Wcm^{-2} and t_{on} = 200 µs (Table 1). A pre-selected critical value of $\bar{I}_d$ = 7.0 A determining the switching-on and switching-off of the oxygen flow rate Φ_{ox} = 16.8 sccm is marked by dots.

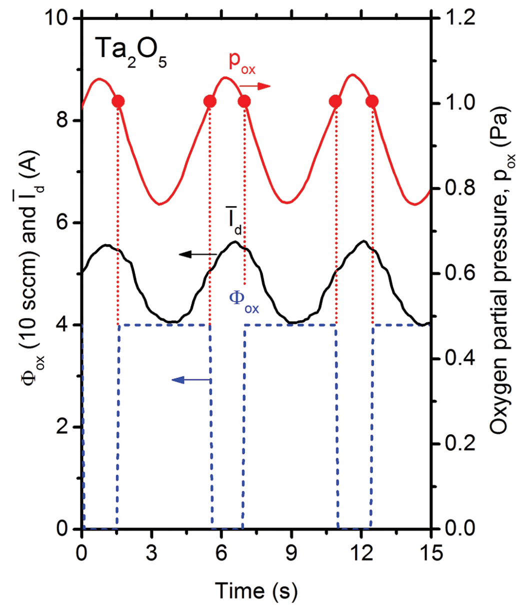

Figure 3. Time evolution of the average discharge current in a period of the power supply, $\bar{I}_d$, oxygen partial pressure, p_{ox}, and the corresponding oxygen flow rate pulses, Φ_{ox}, during a controlled reactive sputter deposition of the stoichiometric Ta_2O_5 film at $<S_d>$ = 53 Wcm^{-2} and t_{on} = 200 µs. A pre-selected critical value of p_{ox} = 1 Pa determining the switching-on and switching-off of the oxygen flow rate Φ_{ox} = 40 sccm is marked by dots.

pulses by means of the pre-selected critical value of $\bar{I}_d(t)$ or $p_{ox}(t)$, which are monitored by the process controller.

A basic principle of the pulsed RGFC is illustrated in Figures 2 and 3. In the depositions of ZrO_2 films, $\bar{I}_d$ is the control process parameter owing to its higher sensitivity, compared with p_{ox}, to Φ_{ox} pulses. In contrast, p_{ox} is the control process parameter in the depositions of Ta_2O_5 films. Under these conditions, the amount of oxygen injected into the discharge is sufficiently low to minimize arcing on the compound part of the metal target and to avoid a substantial reduction in the deposition rate of films, but it is sufficiently high to achieve a sufficient incorporation of the oxygen atoms into the films (stoichiometric composition). A detailed description of the control loop is given in [2].

This feedback process control is able to maintain a sputter deposition of stoichiometric films in the region between a more and less metallic mode and to utilize exclusive benefits of the HiPIMS discharges in the preparation of films [1]. The advantage of the proposed pulsed RGFC method is high stability (no problems with inertia of the inlet system, delay of valves and sensors, and hysteresis effect), simplicity (no additional measurement devices, such as a plasma emission monitoring system, mass spectrometer, or Lambda sensor), and applicability to various power supplies able to keep an approximately constant voltage.

RESULTS AND DISCUSSION

Process and Material Characteristics of Films

Process parameters and material characteristics of stoichiometric ZrO_2 films and HfO_2 films are presented in Tables 1 and 2, respectively. The refractive index, *n*, and extinction coefficient, *k*, were determined by variable angle spectroscopic ellipsometry (using the J.A. Woollam Co. Inc. ellip-

Table 1. Process parameters and material characteristics of stoichiometric ZrO_2 films at preset deposition-averaged target power densities $\langle S_d \rangle$ = 51 - 53 Wcm^{-2}, voltage pulse durations, t_{on}, from 50 to 200 μs, and a fixed argon partial pressure p_{ar} = 2 Pa. The oxygen partial pressures, p_{ox}, were between 0 and 0.08 Pa. Here, S_{da} is the pulse-averaged target power density; U_{da} is the corresponding pulse-averaged magnetron voltage; k_{550} and n_{550} are the extinction coefficient and refractive index of the films at a wavelength of 550 nm, respectively; *H* is the hardness of the films; and *E is their effective Young's modulus.**

Process parameters				Material characteristics			
t_{on} (μs)	$\langle S_d \rangle$ (Wcm^{-2})	S_{da} (Wcm^{-2})	U_{da} (V)	k_{550} (10^{-3})	n_{550}	*H* (GPa)	*E** (GPa)
200	52.0	370–540	484–513	2.0	2.19	16	166
100	51.0	810–1220	528–531	5.0	2.20	16	164
80	53.0	1030–1460	551–542	0.1	1.97	9	135
50	53.0	1700–2100	673–679	1.0	2.07	10	145

Table 2. Process parameters and material characteristics of stoichiometric HfO_2 films at preset deposition-averaged target power densities, $\langle S_d \rangle$, from 29 to 54 Wcm^{-2}, voltage pulse durations, t_{on}, from 50 to 200 μs, and a fixed argon partial pressure p_{ar} = 2 Pa. The oxygen partial pressures, p_{ox}, were between 0.01 and 0.19 Pa. Here, S_{da} is the pulse-averaged target power density; U_{da} is the corresponding pulse-averaged magnetron voltage; k_{550} and n_{550} are the extinction coefficient and refractive index of the films at a wavelength of 550 nm, respectively; *H* is the hardness of the films; and *E is their effective Young's modulus. For comparison, the data obtained for a Hf film prepared at $\langle S_d \rangle$ = 28 Wcm^{-2} and t_{on} = 200 μs are also given.**

Process parameters				Material characteristics			
t_{on} (μs)	$\langle S_d \rangle$ (Wcm^{-2})	S_{da} (Wcm^{-2})	U_{da} (V)	k_{550} (10^{-3})	n_{550}	*H* (GPa)	*E** (GPa)
200	28	280	610	–	–	10	153
200	54	490–630	760–740	1	2.11	18	173
200	33	260–400	630–650	0.5	2.12	18	172
150	29	340–400	655–650	0.6	2.12	18	177
100	30	520–660	700–695	≤ 0.1	2.07	18	173
50	29	1090–1260	895–900	0.5	2.07	15	174

someter). The film hardness, H, and the effective Young´s modulus, $E^* = E/(1-\upsilon^2)$, where E and υ are the Young´s modulus and the Poisson´s ratio, respectively, were determined using an ultramicroindenter (Fischerscope H-100B) according to the ISO 14577-1:2002E standard.

The high values of n_{550} and H prove that the ZrO_2 films (n_{550} = 2.19-2.20 and H = 16 GPa) and the HfO_2 films (n_{550} = 2.11-2.12 and H = 18 GPa), which were prepared at longer voltage pulses, are fully densified. The low values of k_{550} prove that the films (thickness of approximately 1 μm) are highly optically transparent.

Figure 4 shows the range of the waveforms of $U_d(t)$ and $J_t(t)$ during a controlled deposition of the stoichiometric HfO_2 film at $\langle S_d \rangle$ = 33 Wcm^{-2} and t_{on} = 200 μs with the corresponding S_{da} values between 260 and 400 Wcm^{-2} (Table 2). For comparison, the waveforms of $U_d(t)$ and $J_t(t)$ for a Hf film deposition at $\langle S_d \rangle$ = 28 Wcm^{-2} and t_{on} = 200 μs are also given.

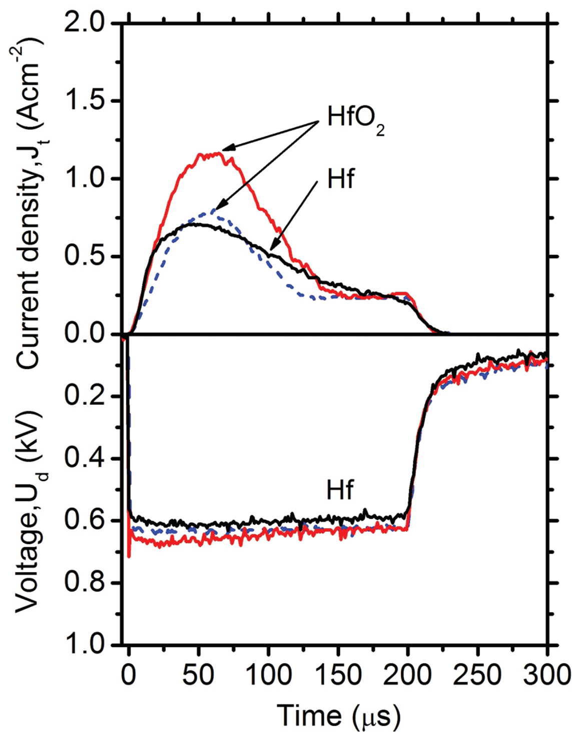

Figure 4. Waveforms of the magnetron voltage, U_d, and the target current density, J_t, relating to the minimum (dashed lines) and maximum (solid lines) values of the average discharge current in a period of the power supply, $\bar{I}_d$, during a reactive sputter deposition of the stoichiometric HfO_2 film at $\langle S_d \rangle$ = 33 Wcm^{-2} and t_{on} = 200 μs (Table 2). Also shown for comparison are the waveforms of U_d and J_t for a Hf film deposition at $\langle S_d \rangle$ = 28 Wcm^{-2} and t_{on} = 200 μs.

High Deposition Rates of Films

Figure 5 shows very high (up to 10 times higher than usual) deposition rates, a_D, achieved for the stoichiometric ZrO_2 and HfO_2. Trends in the measured values of a_D and much higher a_D for the HfO_2 films can be explained using the following simplified equation [3]:

$$a_D \propto (1 - 0.95\theta_{tsa})(1 - B_{ma}) f_{trm} \frac{k_{sp} U_{da}^{-0.5}}{n_{m,c}(1+\gamma)} < S_d >. \quad (4)$$

Here, Θ_{tsa} is the pulse-averaged compound fraction in the target surface layer; B_{ma} is the pulse-averaged probability of ionization and subsequent return of sputtered metal atoms onto the target; f_{trm} is the fraction of sputtered metal atoms, not directed back if ionized, striking the substrate area; k_{sp} is a constant for a given metal in the relation $Y_{mm} = k_{sp}\, U_{da}^{0.5}$ used for the sputtering yield of metal atoms from the metallic fraction of the target [4]; $n_{m,c}$ is the atomic density of the metal atoms in the deposited compound; and γ is the effective ion-induced secondary electron emission yield of the target material.

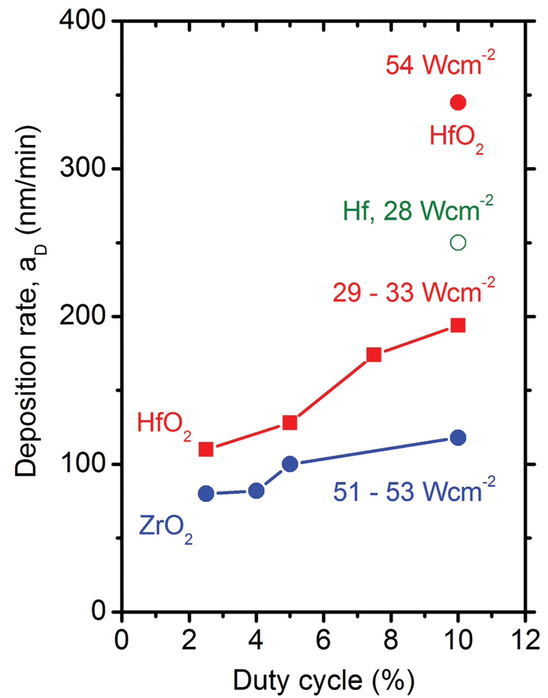

Figure 5. Deposition rates, a_D, of stoichiometric HfO_2 films at deposition-averaged target power densities $\langle S_d \rangle$ = 29 - 33 Wcm^{-2} and various duty cycles ranging from 2.5 % to 10 % (with t_{on} from 50 to 200 μs) and at $\langle S_d \rangle$ = 54 Wcm^{-2} and a duty cycle of 10 % (Table 2). Also presented for comparison are the deposition rates achieved for stoichiometric ZrO_2 films at $\langle S_d \rangle$ = 51-53 Wcm^{-2} and the duty cycle from 2.5% to 10% (Table 1), and for a Hf film prepared at $\langle S_d \rangle$ = 28 Wcm^{-2} and a duty cycle of 10 %.

A shortening of the voltage pulses from 200 μs to 50 μs during the depositions at approximately constant values of $<S_d>$ (see Tables 1 and 2) resulted in rising S_{da}. The rise in S_{da} leads to rapidly increasing probabilities of ionization of sputtered atoms in front of the target. As a consequence, the a_D values decrease mainly due to a higher B_{ma}, which may be combined with a lower f_{trm} (higher losses of the metal ions, compared with neutrals, to chamber walls). Moreover, the values of $U_{da}^{-0.5}$ in equation (4) also decrease, and Θ_{tsa} may be slightly higher for shorter pulses [3]. Systematically higher values of a_D for the HfO_2 films prepared under the same conditions as the ZrO_2 films can be qualitatively explained mainly by a higher f_{trm} at the total pressure close to 2 Pa and by a higher k_{sp} [5].

From equation (4), it is clear that the deposition rate of films achieved using a controlled reactive HiPIMS can be very high at an increased $<S_d>$, allowed by the pulsed RGFC, in spite of an enlarged B_{ma} and U_{da}. The reason is a very low value of Θ_{tsa} (see Figure 6) due to a strong sputtering of reactive gas (RG) atoms from the target surface layer and a strong knock-on implantation of RG atoms from the target surface layer into the target bulk layer [3].

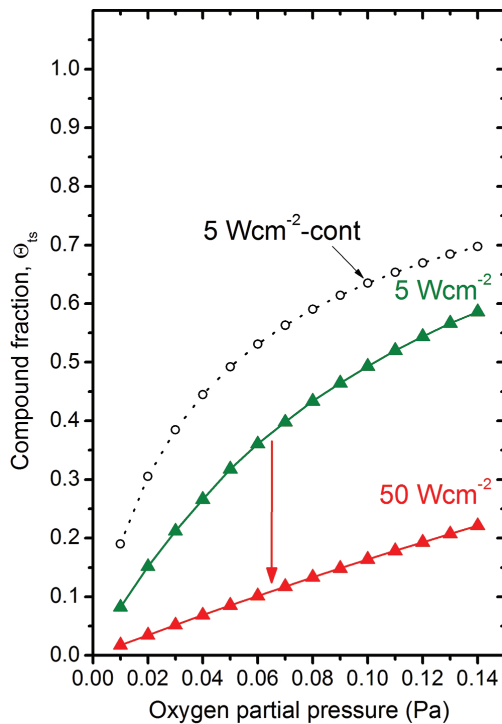

Figure 6. The compound fractions in the target surface layer, Θ_{ts}, calculated for the end of the pulse period T_p = 2000 μs after stabilization of the sputtering process at various fixed oxygen partial pressures, deposition-averaged target power densities $<S_d>$ = 5, and 50 Wcm^{-2}, t_{on} = 200 μs, and p_{ar} = 2 Pa. Also given for comparison are the corresponding stabilized values (circles) of Θ_{ts} obtained for a continuous dc reactive sputtering at a target power density of 5 Wcm^{-2}.

CONCLUSION

A simple and effective pulsed reactive gas flow control for reactive magnetron sputtering of films, which is applicable to various power supplies, was presented. A great potential of the controlled reactive HiPIMS for high-rate deposition of densified dielectric oxide films onto floating substrates at low substrate temperatures was demonstrated. The high deposition rates achieved for the ZrO_2 and HfO_2 films were explained using a simplified formula and model calculations.

ACKNOWLEDGMENT

This work was supported by the Czech Science Foundation under Project No. GA14-03875S.

REFERENCES

1. J. Vlček, J. Rezek, J. Houška, T. Kozák, J. Kohout, "Benefits of the controlled reactive high-power impulse magnetron sputtering of stoichiometric ZrO_2 films", *Vacuum*, 114, p. 131, 2015. https://doi.org/10.1016/j.vacuum.2014.12.004
2. J. Vlček, J. Rezek, J. Houška, R. Čerstvý, R. Bugyi, "Process stabilization and a significant enhancement of the deposition rate in reactive high-power impulse magnetron sputtering of ZrO_2 and Ta_2O_5 films", *Surf. Coat. Technol.*, 236, p. 550, 2013. https://doi.org/10.1016/j.surfcoat.2013.10.052
3. T. Kozák and J. Vlček, "A parametric model for reactive high-power impulse magnetron sputtering of films", *J. Appl. Phys. D: Appl. Phys.*, 49, 055202, 2016. https://doi.org/10.1088/0022-3727/49/5/055202
4. A. Anders, "Self-sputtering runaway in high power impulse magnetron sputtering: the role of secondary electrons and multiply charged metal ions," *Appl. Phys. Lett.*, 92, p. 1, 2008. https://doi.org/10.1063/1.2936307
5. J. Vlček, A. Belosludtsev, J. Rezek, J. Houška, J. Čapek, R. Čerstvý, S. Haviar, "High-rate reactive high-power impulse magnetron sputtering of hard and optically transparent HfO_2 films". *Surf. Coat. Technol.*, 290, p. 58, 2016. https://doi.org/10.1016/j.surfcoat.2015.08.024

FOR MORE INFORMATION:

Jaroslav Vlcek, University of West Bohemia, Department of Physics and NTIS - European Centre of Excellence, Univerzitni 8, 306 14 Plzen, Czech Republic, vlcek@kfy.zcu.cz 420/377632200